Water Qual. Res. J. Canada, 2004 • Volume 39, No. 3, 258–266

Adsorption of As(III) from Aqueous Solution onto Iron Oxide Impregnated Activated Alumina

Shugi Kuriakose, Tony Sarvinder Singh and Kamal K. Pant*

Department of Chemical Engineering, Indian Institute of Technology, Hauz Khas, New Delhi, 110 016, India

The optimal parameters affecting the adsorption of arsenic ions As(III) on iron oxide impregnated activated alumina (IOIAA) were determined by conducting batch and column experiments. The adsorption of As(III) was strongly dependent on pH, temperature and initial adsorbate concentration. The adsorption process satisfied the Langmuir and Freundlich isotherms. Equilibrium studies were conducted to obtain the thermodynamic parameters and data showed the endothermic nature of adsorption. Kinetics studies showed that a pseudo first-order rate equation successfully described the adsorption process. Equilibrium was attained within 10 h and the time taken to attain equilibrium was independent of initial arsenite concentration. Column studies showed that adsorption was strongly dependent on empty bed contact time. Column design parameters such as the time taken for the establishment of primary adsorption zone, fractional capacity, length of primary adsorption zone and the percentage saturation at breakpoint were calculated to be in the range of 18.3 to 70.4 h, 0.39 to 0.63, 3.0 to 3.85 cm and 69.6 to 81.5%, respectively. The observations mentioned above provide a direct relationship between the length of the adsorption zone (δ) and percent saturation at break point.

Key words: **activated alumina, iron oxide, adsorption, arsenite, breakthrough curve**

Introduction

Contamination of drinking water by arsenic has become one of the key environmental health problems of the twenty-first century with new cases of arsenic contamination reported every year. Because of the rapidly accumulating toxicity data, WHO has revised the maximum contaminant limit of arsenic from 50 to 10 µg/L and many countries are following this. Arsenic occurs in groundwater as As(V) (H_3AsO_4, $H_3AsO_4^{1-}$, $HAsO_4^{2-}$) or As(III) (H_3AsO_3, $H_2AsO_3^{1-}$, $HAsO_3^{2-}$). Of these two forms, As(III) is more toxic, difficult to remove and is found in reducing conditions. Most of the developed technologies are effective only when As(V) is the predominant species (Singh et al. 2001). Removal of As(III) has been carried out by converting it to As(V) by oxidation (Driehaus et al. 1995). Oxidizing agents being used for this purpose include manganese oxide (Driehaus et al. 1995), ozone (Kim and Nriagu 2000), and iron (Daus et al. 2000); however residual concentration of these oxidizing agents in water may have toxic effects on human health, thereby limiting their application. Traditionally co-precipitation using lime, ferric salts and alum has been used for arsenic removal but the sludge generation/disposal is a problem. Thus, there is an urgent need for the development of a simple economical and efficient arsenic removal technology.

Most of the adsorbents used for the removal of arsenic can be classified into three major groups, namely, aluminum compounds, lanthanum compounds and iron compounds (Tokunaga et al. 1997). Several studies are available in the literature on goethite, hematite, manganese greensand, iron oxide coated sand (Subramanian et al. 1997; Fendorf et al. 1997; Grossl et al. 1997; Singh et al. 1996; Fe loaded coral limestone, granular ferric hydroxide, pyrite (Ohki et al. 1996; Driehaus et al. 1998; Zouboulis et al. 1992; ferrihydrite (Manceau 1995), activated carbon (2002), hydrotalcite (Manju et al. 2000), and ferruginous manganese ore (Chakravorty et al. 2002). However the arsenic species present in water limits the performance of most of these adsorbents, as most of the available adsorbents are more suited for As(V) removal than As(III). Efforts are also being made to develop a suitable adsorbent for the removal of As(III) from groundwater. Adsorption onto activated alumina has been one of the promising methods for As(V) removal from drinking water but As(III), which is a more mobile and toxic form of arsenic is sometimes difficult to remove by simple activated alumina. Iron(III) oxides have been effectively used for removal of both As(V) and As(III) from aqueous solutions. The occurrence of ferric oxides in the form of fine powder limits the use of ferric oxide in column operations. Adsorption of As(III) by iron oxide coated sand, iron oxide coated granulated activated carbon (Petrusevski et al. 2002), and MnO_2 coated sand (Bajpai and Cahudhari 1999) has been reported in the literature. Vaishya and Aggarwal (1993) showed that sand from the Ganga River (India), which presumably is rich in iron coatings, could remove arsenite from solution, with a reported capacity

* Corresponding author; kkpant@chemical.iitd.ernet.in

of 0.024 mg/g. Joshi and Chaudhuri (1996) reported that iron oxide coated sand (IOCS) was able to remove both arsenite and arsenate. A simple fixed bed unit of IOCS was able to treat about 160 to 190 bed volumes of water containing 1000 µg/L arsenite and 150 to 165 bed volumes of water with 1000 µg/L arsenate. Difficulty in regeneration, non-porous nature, low surface area and high-pressure loss during column runs are some of the disadvantages of using these materials for the removal of arsenic. Generally, the published research work is focussed on the adsorption of As(III) in batch mode. The results of such research work are not strictly applicable for continuous operation. Moreover the adsorption capacity of the sorbents was also low. In the present study, iron oxide impregnated activated alumina was used for the adsorption of As(III) from water in batch and column operations. The objective of the research was to investigate the arsenic(III) removal efficiency of the iron oxide impregnated activated alumina. The effect of parameters such as pH, iron oxide impregnation, adsorbent dose, contact time, and initial solute concentration (C_0) on As(III) adsorption were studied to determine the optimum conditions. Breakthrough studies were carried out to evaluate the performance of the adsorbent in continuous fixed bed operation through changing empty bed contact time by varying flow rate and bed height.

Experimental

Materials

All reagents were prepared using double distilled water. Stock solution of arsenite was prepared using analytical grade sodium arsenite ($NaAsO_2$, Merck, Germany). Working arsenic solutions of different concentrations were prepared by diluting stock arsenic solutions.

Preparation of Adsorbent

Activated alumina (CATAL-AD-101) used in this study was procured from IPCL, Baroda, India. This material has been found effective for the removal of As(V) (Singh and Pant 2004). Ferric sulphate [$Fe_2(SO_4)_3.H_20$, AR Grade, Merck, Germany] was used for impregnation. One hundred grams of activated alumina (AA) pellets were kept in 0.12 M $Fe_2(SO_4)_3.H_20$ solution and placed in an oven at 378 K for 24 h, followed by heat treatment at 878 K for 2 h to set iron oxide coated activated alumina. The ferric sulphate solution was strongly acidic (pH 2.5) due to the hydrolysis of Fe^{3+} ions as shown below.

$$Fe^{+3} + nH_2O \longrightarrow Fe(OH)^{3-n}{}_n + nH^+ \quad (1)$$

During the heat treatment process water evaporated and sulphate was converted to sulphur trioxide, which escaped from the solution, neutralizing and concentrating the residual solution to get ferric oxide to precipitate (Thirunavukkarasu et al. 2001). The final iron oxide content on the AA pellets was 10% (by weight). These pellets were characterized for their surface area, pore volume and other properties. The surface area and pore volume measurements were carried out using BET surface area and pore volume analyzer (Micromeritics ASAP 2010 USA). The physico-chemical properties of AA before and after impregnation with iron oxide are shown in Table 1. It was found that there was a significant reduction in surface area and pore size as a result of iron oxide diffusion into the pores of the AA (Table 1).

Arsenic Analysis

Arsenic analysis was carried out using a Varian Spectra AA 880 graphite furnace atomic absorption spectrometer (GF-AAS Varian, Australia), with Zeeman background correction. All measurements were based on integrated absorbance and performed at 193.7 nm by using a hollow cathode lamp (Varian, Australia). Pretreatment temperature of the furnace was 1400 K and atomization temperature was 2500 K. The calibration range was 20 to 100 µg L^{-1} of arsenic.

Batch Study

A comparative study for the effectiveness of iron oxide impregnated AA and AA (without impregnation) for the As(III) removal was conducted. Batch experiments were carried out in a temperature controlled mechanical shaker (Neolab instruments, Mumbai, India). Solution pH is an important factor for all water and wastewater treatment processes as it affects the speciation of the metals. Studies were conducted at different initial pH levels (3.0–12.0) to determine the effect on As(III) adsorption, 50 gL^{-1} of iron oxide impregnated AA was added to different flasks each containing As(III) solution. These samples were agitated in a mechanical shaker at 85 rpm and 298 K until equilibrium was reached. Samples were filtered through Whatman no.1 filter paper and the residual As(III) concentration was determined.

TABLE 1. Physical properties of adsorbents

Properties	*Activated alumina*	*Iron oxide impregnated activated alumina (IOIAA)*
Particle form	Spheres	Spheres
Colour	White	Reddish brown
Particle size (mm)	2.0 ± 0.2	2.0 ± 0.2
Surface area (m^2/g)	365 ± 5	200 ± 10
Pore volume (cm^3/g)	0.42	0.27
Bulk density (g/cm^3)	0.800	0.850

Equilibrium Study

Different weights of adsorbent (0.1–5.0 g) were added to 500-mL conical flasks, each filled with 100 mL of As(III) solution (C_0 1.4 mg/L) and allowed to equilibrate for 24 h to reach equilibrium at the desired temperature (298, 308 and 315 K). Residual arsenic concentration was determined in each sample.

Kinetic studies were conducted with different initial As(III) concentrationsranging from 1.6 to 2.3 mg/L. Iron oxide impregnated AA pellets (5.0 g) were suspended in 100 mL of As(III) solution at pH 12.0 in different conical flasks in a shaker at 85 rpm. Samples withdrawn at regular time intervals were filtered and analyzed for residual As(III) concentration.

Column Experiments

A Perspex column (45 cm length and 2.5 cm internal diameter) was used as a vertical fixed bed column. An overhead water reservoir with constant head and fitted with a flow control valve was placed over the column through which arsenic solution was allowed to pass. Fixed bed studies were conducted to evaluate column performance at optimum pH 12.0. Contact time was varied from 4 to 18 min by varying inlet flow rate and bed height. Samples were collected at regular intervals at the exit of the column and analyzed.

Results and Discussion

Effectiveness of Iron Oxide Impregnation

The performance of iron oxide impregnated AA (IOIAA) was compared with AA for the removal of As(III). The As(III) uptake plotted as a function of the equilibrium concentration is shown in Fig. 1. Iron oxide coating results in an increase in the percentage adsorption of solute. Compared to AA, the As(III) uptake increased from 0.158 to 0.286 mg/g with iron oxide impregnation. A higher value of q_e for iron oxide impregnated AA compared to AA confirmed that impregnation resulted in an increased sorption of As(III). Higher adsorption was achieved most probably due to enhancement in the rate of reaction. Cation (available in solution) adsorption and columbic interaction play a major role in the adsorption of As(III) on IOIAA. Formation of ferric arsenite could be another mechanism responsible for this. Ferric arsenite formation by the following reaction has also been reported elsewhere (Katsoyiannis and Zouboulis 2002).

$$\text{M-FeOH} + H_3AsO_3 \rightarrow \text{M-Fe-}H_2AsO_3 + H_2O \quad (2)$$

Effect of Solution pH on As(III) Adsorption

The percentage of As(III) removed at various initial pH levels for arsenic concentration of 1.1 mg/L is shown in Fig. 2. It was observed that the percentage of As(III) removal was least affected (78–83%) in the pH range of 3 to 8. Increasing pH beyond 8.0, there was a significant increase in the As(III) removal and maximum As(III) removal (96.7%) was obtained at a pH of 12.0. The solubility of activated alumina and IOIAA used in the present study at pH 12 were less than 0.5% (by wt.) and 0.2% (by wt.), respectively.

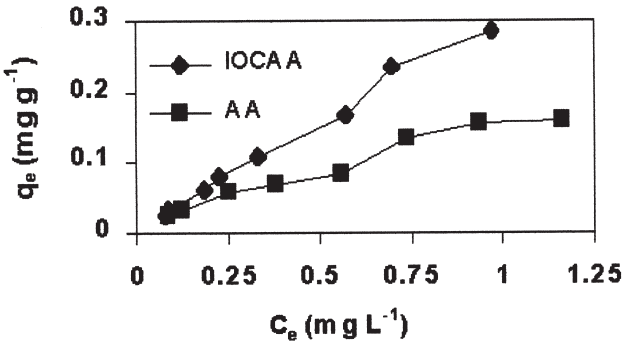

Fig. 1. Effect of iron oxide coating on As(III) adsorption (pH 12.0, adsorbent dose 5 g/100 mL; C_0 1.0 mg/L).

Several investigators reported maximum As(III) removal in an alkaline pH range by different sorbents such as red mud (Altundogan et al. 2000) and hydrotalcite (Manju and Anirudhan 2000). Manju et al. (1998) also reported that As(III) adsorption on coconut husk carbon increased from 16 to 86% as pH was increased from 3 to 12. In contrast to the results obtained for iron oxide impregnated AA, a pH value of 7.6 was found to be optimum for AA (Singh and Pant 2004). The difference in optimum pH in the case of IOIAA and AA for maximum As(III) removal could be attributed to the difference in surface characteristics of both adsorbents. The higher removal in the basic medium could be due to the presence of As(III) as anionic species $H_2AsO_3^-$. Under the condition of pH less than 9.2, non-ionic H_3AsO_3 is the dominant species and therefore the only force acting between H_3AsO_3 and the surface is the weaker van der

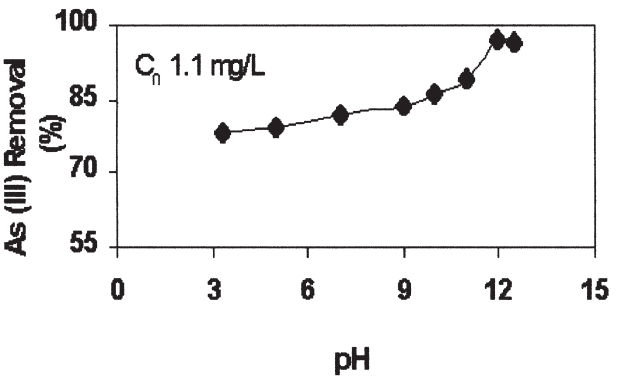

Fig. 2. Effect of pH on As(III) adsorption (C_0 1.1 mg/L; adsorbent dose 50 g/L; temperature 298 K).

Waals force. At a higher pH the dominant species is negatively charged leading to a higher adsorption. It should be noted that although optimal removal was achieved at pH 12.0, the treated water pH at the end of the experimental run was 7.3, which is suitable for drinking without any further post treatment.

Adsorption Isotherms

Adsorption isotherm data are quantified to describe the interactions between the adsorbate and adsorbent and are critical in optimizing the use of adsorbent. The Langmuir equation is the most popular of all the nonlinear isotherm expressions; it is a two-parameter equation:

$$q_e = \frac{bq_mC_e}{1 + bC_e} \tag{3}$$

where constants b and q_m relate to the energy of adsorption and adsorption capacity and their values were obtained from the slope and intercept of the plot of $1/q_e$ versus $1/C_e$ (Fig. 3). The linear nature of the plot shows that the adsorption follows the Langmuir isotherm and the increase in temperature from 298 to 315 K resulted in an increase of about 17% in adsorption capacity (Table 2). The value of b, which is a measure of heat of adsorption, also increased with an increase in temperature. Lin et al. (2001) obtained similar results for arsenite adsorption on AA and found q_m to be in the range 0.76 to 2.29 mg/g and b in the range 0.77 to 1.24 L/mg.

The Freundlich isotherm equation for representing equilibrium data, is given by:

$$q_e = kC_e^{\frac{1}{n}} \tag{4}$$

where k and n are Freundlich constants corresponding to adsorption capacity and adsorption intensity, respectively. The slope (1/n) and intercept (k) of a log-log plot of q_e versus C_e as determined from Fig. 4 are tabulated in Table 2. An increase in temperature resulted in an increase in k and n indicating increased capacity and intensity of adsorption. Similar results have been reported for arsenite adsorption on red mud and coconut husk carbon (Altundogan et al. 2000; Manju et al. 1998).

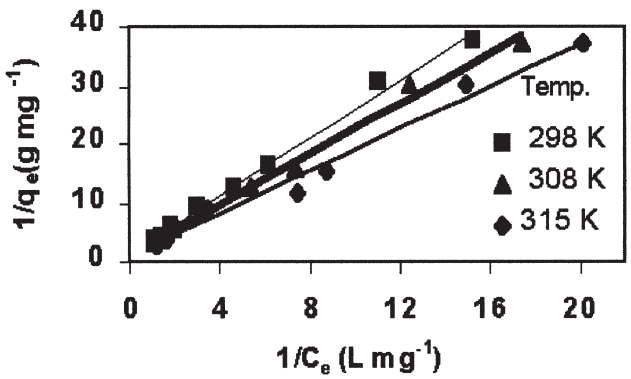

Fig. 3. Plot of Langmuir adsorption isotherm (pH 12.0; C_0 1.4 mg/L; rpm 85).

As(III) removal increased with an increase in temperature showing the endothermic nature of the process. Thermodynamic parameters were also evaluated to confirm the endothermic nature of the process. The thermodynamic constants, Gibb's free energy (ΔG^o), enthalpy change (ΔH^o) and entropy change (ΔS^o) were calculated to evaluate the thermodynamic feasibility of the process and to confirm the nature of the adsorption process. The Gibb's free energy change of the process is related to equilibrium constant (k_0) by equation 6:

$$\Delta G^o = -RT \ln K_o \tag{5}$$

The Gibb's free energy change is related to the enthalpy change (ΔH^o) and entropy change (ΔS^o) as:

$$\ln K_o = \frac{\Delta S^o}{R} - \frac{\Delta H^o}{RT} \tag{6}$$

where K_o is equilibrium constant (m^3mol^{-1}) which was calculated from the Langmuir constant b. The values of enthalpy change (ΔH^o) and entropy change (ΔS^o) were calculated from the slope and intercept of the plot of ln K_o versus 1/T (Fig. 5). The parameters as calculated are also reported in Table 2. The negative ΔG^o value confirmed the feasibility of the sorption process and the spontaneous nature of adsorption. The positive value of ΔH^o obtained indicated the endothermic nature of the process. The positive ΔS^o value indicated the affinity of the adsorbent for As(III).

Kinetics Study

The kinetics of As(III) adsorption on iron oxide impregnated AA was studied at different initial concentrations of As(III) (1.6–2.3 mg/L) as a function of time at 298 K and the results are shown in Fig. 6 which is a plot of residual As(III) concentration as a function of contact time. The uptake of As(III) increased with an increasing contact time, however the adsorption rate was rapid in the first four hours. Equilibrium was attained in approximately 10 h after which the amount of residual As(III) in solution remained practically unchanged. For an initial As(III) concentration of 1.6 mg/L the equilibrium uptake of As(III) was 30 mg/kg and increased to 44.0 mg/kg when the initial concentration was increased to 2.3 mg/L. In the present study, the maximum adsorption capacity with iron oxide impregnated AA was 378 mg/kg from a water having initial As(III) concentration of 1.4 mg/L. This is significantly higher than that estimated for iron oxide coated sand (18.3 µg/g) and ferrihydrite (285 µg/g) for arsenic removal (Thirunavukkarasu et al. 2001).

TABLE 2. Adsorption isotherm and thermodynamic parameters

Temperature (K)	Langmuir isotherm constant			Freundlich isotherm constant			K_o x 10^{-3} (m^3 mol^{-1})	$-\Delta G^o$ (kJ mol^{-1})	ΔH^o (kJ mol^{-1})	ΔS^o (kJ mol^{-1} K^{-1})
	b (L/mg)	q_m (mg/g)	R^2	k (mg/g)	n	R^2				
298	0.554	0.734	0.993	0.302	1.113	0.996	41.5	26.34	6.82	0.111
308	0.584	0.803	0.990	0.344	1.114	0.992	43.8	27.36		
315	0.646	0.858	0.984	0.374	1.160	0.980	48.4	28.25		

The nature of adsorption kinetics was determined using the Lagergren equation given below (**Lagergren 1898**):

$$\log (q_e - q_t) = -\frac{k_{ad1} t}{2.303} + \log (q_e) \quad (7)$$

where k_{ad1} is the rate constant of the first-order adsorption (h^{-1}) and q_e and q_t are the amount of As(III) adsorbed per unit mass of adsorbent (mg/g) at equilibrium and at time, t, respectively. It was noted that a semi-log plot of (q_e-q_t) as a function of time yields a straight line (Fig. 7) showing that the adsorption process followed the first-order kinetics at lower As(III) concentration. The value of the adsorption rate constants, k_{ad}, were obtained from the slope of Fig. 8 with the regression coefficients more than 0.95. The first-order rate constant (k_{ad1}) varied from 1.0 to 1.42 h^{-1} as concentration was increased from 1.6 to 2.3 mg/L. There was a considerable increase in the first-order rate constant at higher As(III) concentration, so a pseudo second-order rate constant was also applied which showed that the adsorption rate constant followed a pseudo second order at a higher concentration (Table 3).

Besides adsorption on the outer surface of the adsorbent, there is also a possibility of transport of adsorbate ions from the solution into the pores of the sorbent due to the rapid stirring in the batch reactor. The experimental data could be used to study the rate-limiting step in the adsorption process. Since the particles are vigorously agi-

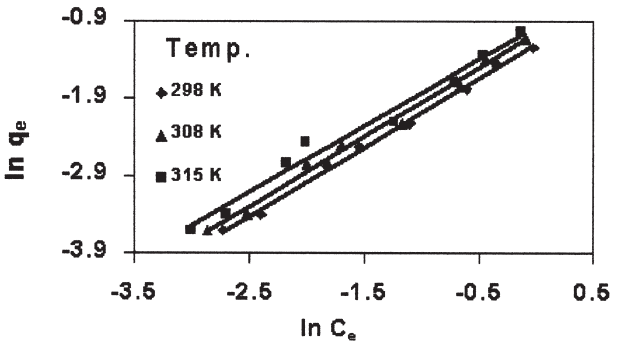

Fig. 4. Plot of Freundlich adsorption isotherm (pH 12.0; C_0 1.4 mg/L; rpm 85).

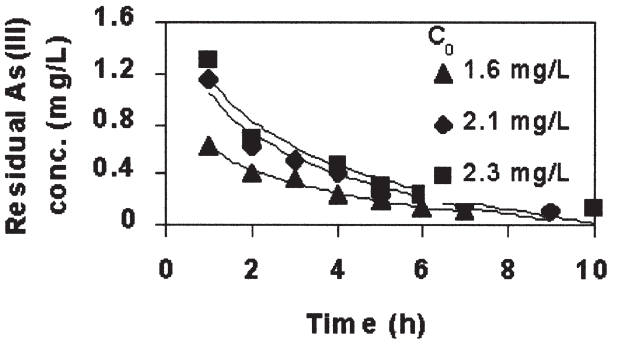

Fig. 6. Residual As(III) concentration as a function of contact time (pH 12.0; adsorbent dose 50 g/L; temperature 298 K).

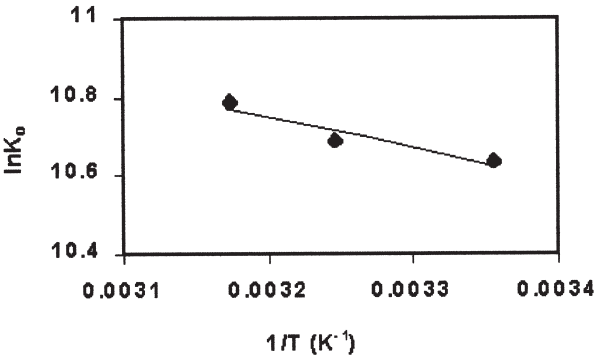

Fig. 5. Estimation of thermodynamic parameters (pH 12.0; C_0 1.4 mg/L; rpm 85).

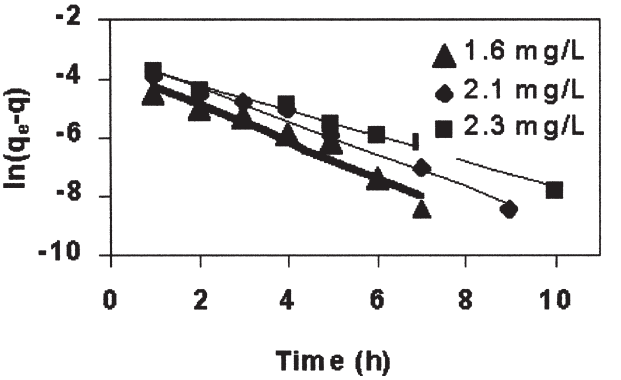

Fig. 7. Evaluation of first-order rate constants (pH 12.0; adsorbent dose 50 g/L; temperature 298 K).

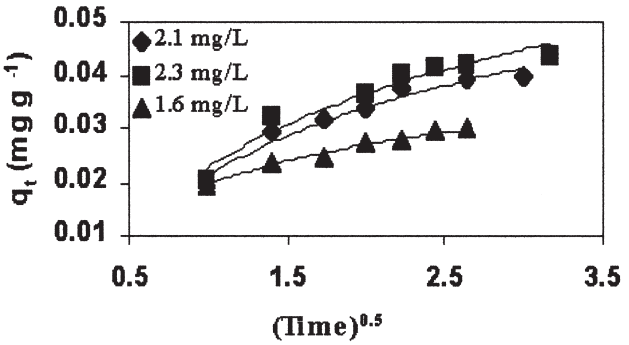

Fig. 8. Estimation of intra particle diffusion rate constants (pH 12.0; adsorbent dose 50 g L^{-1}; temperature 298 K).

tated during the adsorption, it is reasonable to assume that the mass transfer from the bulk liquid to the particle external surface does not limit the rate. Hence, it can be postulated that the rate-limiting step may be intraparticle diffusion. As these act in series, the slower of the two will be the rate-limiting step. The rate constant for intraparticle diffusion is obtained using the equation (Al-Asheh et al. 2003):

$$q = k_p t^{0.5} \quad (8)$$

where k_p (mg g^{-1} h$^{-0.5}$) is the intraparticle diffusion rate constant. The dual nature of these plots (Fig. 8) may be explained as the initial curved portions are attributed to boundary layer diffusion effects while the final linear portions are due to intraparticle diffusion effects. The intraparticle diffusion rate constant, k_p, at different initial concentrations (Table 3) were determined from the slope of the linear portion of the respective plots. The initial As(III) concentration of the solution did not influence the adsorption rate constants significantly (Table 3). The intraparticle diffusion rate constants were found to vary from 0.02 to 0.03 mg g^{-1} h$^{-0.5}$ with an increase in initial As(III) concentration from 1.6 to 2.3 mg/L.

Column Studies

An idealized breakthrough curve is expressed by plotting mass concentration of solute in the effluent, C_t, and the total mass quantity of solute-free water, V_{eff}, which has passed a unit cross-sectional area of the adsorber. The breakthrough point was chosen at a C_b value of 0.01 mg/L. Adsorption of As(III) was studied at the flow rates of 120 and 300 mL/h. The influent As(III) concentration was maintained at 0.5 mg/L for these experiments. The breakthrough plots of C_t/C_0 against volume of effluent treated at an arsenic concentration of 0.5 mg/L at different flow rates are shown in Fig. 9 and 10.

As can be seen from Fig. 9 and 10, an increase in breakthrough time with a decrease in the flow rate was observed. This is probably due to the availability of sorption sites to capture metal ion around or within the IOIAA pellet. With the gradual occupancy of these sites, the uptake of As(III) became less effective. As the flow rate increased, the breakthrough curve becomes steeper. The empty bed contact time (EBCT) of 9.4 and 3.7 min corresponding to flow rates of 2 and 5 mL/min were taken for column runs. With a higher EBCT, metal ions had more time to contact with IOIAA, which resulted in higher removal of As(III) ions in fixed-bed columns. A high decrease in sorbate concentration can be attributed to the fact that residence time for the solute in the column was sufficiently high enough for adsorption equilibrium to be reached at that flow rate. At a higher flow rate, reduction in As(III) removal efficiency has been observed.

The effect of residence time was also studied by varying the bed height under identical conditions. Experiments were conducted at a column bed height of 6 and 12 cm corresponding to residence times of 9.4 and 18.8 min, respectively. As(III) ions were passed through the column at a flow rate for 120 mL/h with an initial As(III) concentration of 0.5 mg/L. The results are shown in Fig. 10. At a lower contact time, the curve is steeper showing the faster exhaustion of the fixed bed.

Analysis of Breakthrough Data

Breakthrough capacity of the fixed bed was determined by plotting exit As(III) concentration, C_t, against volume of water treated (V). Mass units for C and V_e were used to illustrate the concept of mass balance. Nature of the breakthrough curve between V_b and V_x and the quantities of effluent treated per unit cross section till breakthrough are primary parameters for the designing of a fixed bed adsorber (Gupta et al. 2000).

The time required for movement of PAZ onwards in the column (t_δ) can be calculated as:

$$t_\delta = \frac{V_x - V_b}{F_m} \quad (9)$$

TABLE 3. Intraparticle diffusion and reaction rate constants adsorption of As(III) on IOIAA

Initial As(III) conc. (mg/L)	k_{ad1} (h^{-1})	R^2	K_{ad2} $(mg/g)^{-1}$ min^{-1}	R^2	k_p (mg g^{-1} h$^{-0.5}$)
1.6	1.4	0.934	0.62	0.98	0.022
2.1	1.3	0.981	0.28	0.987	0.032
2.3	1.0	0.986	0.28	0.987	0.035

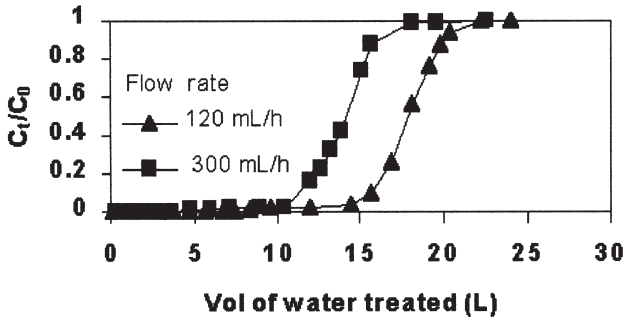

Fig. 9. Breakthrough curves at different flow rate (bed height 6 cm; C_0 0.5 mg/L; pH 12).

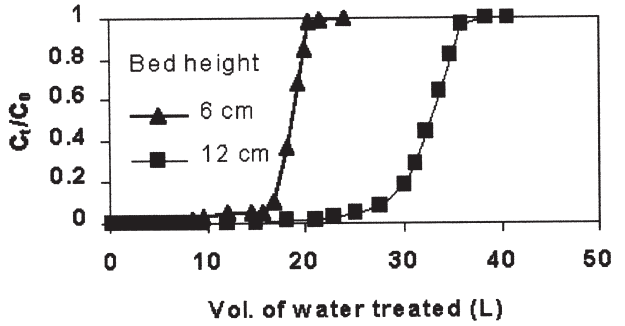

Fig. 10. Effect of bed height on shape of breakthrough curve (2 mL min^{-1}, C_0 0.5 mg/L).

Fractional capacity, f, of IOIAA in the adsorption zone at breakpoint to continue to remove solute from solution under the limiting conditions is given by:

$$f = \frac{M_s}{C_O(V_x - V_b)} \tag{10}$$

Thus, for a depth D of the IOIAA bed, the depth and time ratios may be equated as:

$$\frac{\delta}{D} = \frac{t_\delta}{t_x - t_f} \tag{11}$$

where t_f represented the time required for initial formation of the PAZ. The percent saturation was calculated as:

$$\% \text{ saturation} = [1 - \frac{\delta(1-f)}{D}] \times 100 \tag{12}$$

The values of V_b, V_x, C_b and C_x were obtained from breakthrough curves and the values are listed in Table 4. These values were used to calculate t_x, t_δ, t_f, δ, f and % saturation (Table 5) at different EBCT at a bed height of 6 cm and an initial As(III) concentration of 0.5 mg/L. As can be seen in Table 5 the time taken for the initial formation of PAZ varied from 18.3 to 70.4 h. The percent saturation at breakpoint also depended on EBCT and varied from 69.6 to 81.5. These observations provide a direct relationship between length of adsorption zone and percent saturation at breakpoint. The smaller the length of the adsorption zone, the lower the percentage saturation observed will be. These operation parameters may be helpful in designing a fixed bed adsorber for the removal of arsenic ions of a known concentration.

Conclusions

The following conclusions were drawn from the present study.

1. Iron oxide impregnated activated alumina was found to be an effective adsorbent for the removal of As(III). Compared to activated alumina there was significant enhancement in adsorption capacity.
2. Adsorption was strongly dependent on initial pH and initial As(III) concentration. Maximum adsorption (96.7%) was achieved at pH 12.
3. The adsorption process followed first-order kinetics at the lower As(III) concentrations (up to 2.1 mg/L). At higher As(III) concentration, the behaviour was accurately explained by pseudo second-order rate kinetics.

TABLE 4. Observed parameters for fixed bed adsorption of As(III) on IOIAA

EBCT (s)	*C_0 (mg/L)*	*C_x (mg/L)*	*C_b (mg/L)*	*V_x (g/cm^2)*	*V_b (g/cm^2)*	*V_x-V_b (g/cm^2)*	*F_m (g/h/cm^2)*	*D (cm)*
222	0.5	0.49	0.01	3971	2138	1833	61.0	6
564	0.5	0.49	0.01	4521	2444	2077	24.4	6
1128	0.5	0.49	0.01	5499	3177	2322	12.2	6

TABLE 5. Calculated parameters for fixed bed adsorption of As(III) on IOIAA

EBCT (s)	*t_x (h)*	*t_δ (h)*	*f*	*t_f (h)*	*δ (cm)*	*% Saturation*
222	65.0	30.0	0.39	18.3	3.85	69.6
564	185.2	85.1	0.55	38.2	3.19	76.0
1128	450.7	190.3	0.63	70.4	3.0	81.5

4. Experimental data satisfactorily fit Langmuir and Freundlich isotherms. Higher adsorption was observed at higher temperatures indicating the endothermic nature of adsorption.
5. The breakthrough curves for adsorption of As(III) showed the mutual effects of adsorption capacity and adsorption rate. The shape of breakthrough curve obtained was a strong function of flow rate and bed height of the sorbents bed. The percent saturation was lower for the smaller length of adsorption zone. The parameters obtained from this study can be used to establish the time required for breakthrough to occur and additional solution required per unit cross-sectional area of adsorber in the complete exhaustion of the bed.

Acknowledgement

We are thankful to the UGC (University Grants Commission), New Delhi, India, for providing financial support for the research.

References

Al-Asheh S, Banat F, Abu-Aitah L. 2003. Adsorption of phenol using different types of activated Bentonites. Separat. Purif. Technol. **3:**1–10.

Altundogan HS, Altundogan S, Tumen F, Bildik M. 2000. Arsenic removal from aqueous solutions by adsorption on red mud. Waste Manage. **20:**761–767.

Bajpai S, Chaudhuri M. 1999. Removal of arsenic from ground water by manganese dioxide-coated sand. J. Environ. Eng. **125:**782–784.

Chakravorty S, Dureja V, Bhattacharya G, Maity S, Bhattacharjee S. 2002. Removal of arsenic from groundwater using low cost ferruginous manganese ore. Water Res. **36:**625–632.

Daus B, Mattusch J, Paschke A, Wennrich R, Weiss H. 2000. Kinetics of the arsenite oxidation in seepage water from a tin mill tailings pond. Talanta **51:**1087–1095.

Driehaus W, Jekel M, Hildebrand U. 1998. Granular ferric hydroxide—a new adsorbent for the removal of arsenic from natural water. J. Water SRT–Aqua **47:**30–35.

Driehaus W, Seith R, Jekel M. 1995. Oxidation of arsenate(III) with manganese oxides in water treatment. Water Res. **29:**297–305.

Fendorf SM, Eick J, Grossl PR, Sparks DL. 1997. Arsenate and chromate retention mechanisms on goethite. I. Surface structure. Environ. Sci. Tech. **31:**315–320.

Grossl PR, Eick MJ, Sparks DL, Goldberg S, Ainsworth CC. 1997. Arsenate and chromate adsorption/desorption on goethite. II. Kinetic evaluation using a P-jump relaxation technique. Environ. Sci. Tech. **31:**321–326.

Gupta VK, Srivastava SK, Tyagi R. 2000. Design parameters for the treatment of phenolic wastes by carbon columns obtained from fertilizer waste material. Water Res. **34(5):**1543–1550.

Joshi A, Chaudhuri M. 1996. Removal of arsenic from ground water by iron oxide-coated sand. J. Environ. Eng. **122:**769–772.

Katsoyiannis IA, Zouboulis AI. 2002. Removal of arsenic from contaminated water sources by sorption onto iron-oxide-coated polymeric materials. Water Res. **36:**5141–5155.

Kim MJ, Nriagu J. 2000. Oxidation of arsenite in groundwater using ozone and oxygen. Sci. Total Env. **247:** 71–79.

Lagergren S. 1898. About the theory of so-called adsorption of soluble substances. K. Sven. Vetenskapsakad Handl. **24:**1–39.

Lin TF, Wu JK. 2001. Adsorption of arsenite and arsenate within AA grains: equilibrium and kinetics. Water Res. **35:**2049–2057.

Manceau A. 1995. The mechanism of anion adsorption on iron oxides: evidence for the bonding of arsenate tetrahedra on free Fe(OOH) edges. Geochimica et Cosmochimica Acta **59:**3647–3653.

Manju GN, Anirudhan TS. 2000. Treatment of arsenic(III) containing wastewater by adsorption on hydrotalcite. Ind. J. Environ. Health **42:**1–8.

Manju GN, Raji C, Anirudhan TS. 1998. Evaluation of coconut husk carbon for the removal of arsenic from water. Water Res. **32:**3062–3070.

Nagarnaik PB, Bhole AG, Natarajan GS. 2002. Arsenic (III) removal by adsorption on rice husk carbon. Int. J. Environ. Studies **5:**97–102.

Ohki A, Nakayachigo K, Naka K, Maeda S. 1996. Adsorption of inorganic and organic arsenic compounds by aluminum-loaded coral limestone. Appl. Organmetal. Chem. **10:**747–752.

Petrusevski B, Boere J, Shahidullah SM, Sharma SK, Schippers JC. 2002. Adsorbent-based point-of-use system for arsenic removal in rural areas. Water SRT–Aqua **51:** 135–144.

Singh DB, Prasad G, Rupainwar DC. 1996. Adsorption technique for the treatment of As(V)-rich effluents. Colloids Surf. A **111:**49–56.

Singh P, Singh TS, Pant KK. 2001. Removal of arsenic from drinking water using activated alumina. Res. J. Chem. Environ. **5:**25–28.

Singh TS, Pant KK. 2004. Equilibrium, kinetics and thermodynamic studies for adsorption of As(III) on activated alumina. Sep. Pur. Technol. **36:**139–147.

Subramaniam KS, Viraraghavan T, Phommavong T, Tanjore S. 1997. Manganese greensand for removal of arsenic in drinking water. Water Qual. Res. J. Canada **32:**551–561.

Thirunavukkarasu OS, Viraraghavan T, Subramaniam KS. 2001. Removal of arsenic in drinking water by iron oxide-coated sand and ferrihydrite - batch studies. Water Qual. Res. J. Canada **36:**55–70.

Thirunavukkarasu OS, Viraraghavan T, Subramanian KS. **2003a. Arsenic removal from drinking water using iron oxide coated sand. Water Air Soil Pollut.** 142:**95–111.**

Thirunavukkarasu OS, Viraraghavan T, Subramanian KS. **2003b. Arsenic removal from drinking water using granular ferric hydroxide. Water SA** 29:**161–170.**

Tokunaga S, Wasay SA, Park SW. 1997. Removal of arsenic(V) ion from aqueous solutions by lanthanum compounds. Water Sci. Tech. **35:**71–78.

Vaishya RC, Aggarwal IC. 1993. Removal of arsenic(III) from contaminated ground waters by Ganga sand. J. Ind. Water Works Assoc. **25:**249–253.

Zouboulis AI, Kydros KA, Matis KA. 1992. Adsorbing flotation of copper hydroxo-precipitates by pyrite fines. Sep. Sci. Tech. **27:**2143–2155.

Received: October 23, 2003; accepted: June 14, 2004.

Nomenclature

b	Langmuir constant (L/mg).
C	Arsenic concentration in solution (mg/L).
C_0	Initial As(III) concentration (mg/L).
C_b	Effluent sorbate concentration at breakthrough (mg/L).
C_e	Equilibrium As(III) concentration (mg/L).
C_x	Effluent sorbate concentration at bed saturation (mg/L).
D	Bed height (cm).
δ	Length of primary adsorption zone (cm).
f	Fractional capacity of IOIAA column.
F_m	Mass flow rate (g cm^2 h^{-1}).
ΔG	Gibb's free energy change (kJ/mol).
ΔH	Enthalpy change (kJ/mol).
ΔS	Entropy change (kJ $mol^{-1}K$).
k	Freundlich constant (mg/g).
K	Temperature (Kelvin).
k_{ad1}	First-order rate constant (h^{-1}).
k_{ad2}	Second-order rate constant (mg g^{-1} min^{-1}).
K_o	Equilibrium constant (m^3/mol).
k_p	Intraparticle diffusion coefficient (mg g^{-1} $min^{-0.5}$).
M_s	Amount of solute adsorbed by sorbent in PAZ from breakthrough to exhaustion (g).
n	Freundlich constant (dimensionless).
q	Amount of As(III) adsorbed per unit mass of adsorbent (mg/g).
q_e	Amount of As(III) adsorbed per unit mass of adsorbent at equilibrium (mg/g).
q_m	Maximum monolayer capacity (mg/g).
q_t	Amount of As(III) adsorbed per unit mass of adsorbent at time t (mg/g).
R	Gas constant (kJ mol^{-1}).
t	Time (s).
T	Temperature (K).
t_δ	Time required for movement of PAZ downward the column (h).
t_f	Time required for initial formation of PAZ (h).
t_x	Total time taken for primary adsorption zone (PAZ) to establish and move down length of column (h).
V	Volume of water sample per unit cross-sectional area of the bed (g cm^{-2}).
V_b	Volume of effluent treated till breakthrough per unit cross-sectional area of the bed (g cm^{-2}).
V_x	Volume of effluent treated per unit cross-sectional area of the bed till saturation (g cm^{-2}).
W	Weight of adsorbent (g).